

Published in final edited form as:

*Biomacromolecules*. 2013 April 8; 14(4): 1085–1092. doi:10.1021/bm3019856.

## Synthesis and Characterization of Hybrid Hyaluronic Acid-Gelatin Hydrogels

Gulden Camci-Unal<sup>1,2</sup>, Davide Cuttica<sup>1,2,3</sup>, Nasim Annabi<sup>1,2,4</sup>, Danilo Demarchi<sup>3,5</sup>, and Ali Khademhosseini<sup>1,2,4,\*</sup>

<sup>1</sup>Center for Biomedical Engineering, Department of Medicine, Brigham and Women's Hospital, Harvard Medical School, Cambridge, MA 02139, USA

<sup>2</sup>Harvard-MIT Division of Health Sciences and Technology, Massachusetts Institute of Technology, 77 Massachusetts Avenue, Cambridge, MA 02139, USA

<sup>3</sup>Politecnico di Torino, Torino, Italy

<sup>4</sup>Wyss Institute for Biologically Inspired Engineering, Harvard University, Boston, MA 02115, USA

<sup>5</sup>Department of Electronics and Telecommunications, Politecnico di Torino, Torino, Italy

### Abstract

Biomimetic hybrid hydrogels have generated broad interest in tissue engineering and regenerative medicine. Hyaluronic acid (HA) and gelatin (hydrolyzed collagen) are naturally derived polymers and biodegradable under physiological conditions. Moreover, collagen and HA are major components of the extracellular matrix (ECM) in most of the tissues (e.g. cardiovascular, cartilage, neural). When used as a hybrid material, HA-gelatin hydrogels may enable mimicking the ECM of native tissues. Although HA-gelatin hybrid hydrogels are promising biomimetic substrates, their material properties have not been thoroughly characterized in the literature. Herein, we generated hybrid hydrogels with tunable physical and biological properties by using different concentrations of HA and gelatin. The physical properties of the fabricated hydrogels including swelling ratio, degradation, and mechanical properties were investigated. In addition, *in vitro* cellular responses in both two and three dimensional (2D and 3D) culture conditions were assessed. It was found that the addition of gelatin methacrylate (GelMA) into HA methacrylate (HAMA) promoted cell spreading in the hybrid hydrogels. Moreover, the hybrid hydrogels showed significantly improved mechanical properties compared to their single component analogs. The HAMA-GelMA hydrogels exhibited remarkable tunability behavior and may be useful for cardiovascular tissue engineering applications.

### Keywords

hyaluronic acid; gelatin; hydrogel; extracellular matrix; tissue engineering

## 1. INTRODUCTION

Hydrogel-based scaffolds have been commonly used in regenerative engineering research to replace defective, degenerated or damaged tissues.<sup>1, 2</sup> Hydrogels are crosslinked 3D

\*Correspondence should be addressed to: Ali Khademhosseini (alik@rics.bwh.harvard.edu).

### Author Contributions

GC-U and AK designed the experiments and GC-U synthesized the methacrylated hydrogels. GC-U and DC performed the experiments and analyzed the data. GC-U wrote the paper. GC-U, DC, NA, DD, and AK revised and commented on the manuscript. All authors checked and approved the contents of the manuscript.

networks that are composed of highly hydrophilic polymers. The ability to generate 3D flexible matrices allows for studying cell-cell and cell-biomaterial interactions in a controlled manner. For this reason, synthesizing hydrogels from materials that are derived from native extracellular matrix (ECM) molecules is a popular approach to synthesize biomimetic materials. Hydrogels can potentially mimic the native ECM environment by their soft and flexible structures and high water content. Therefore, they are widely used for both surface seeding and 3D cell encapsulation to form biomimetic constructs. Cell-laden hydrogel systems have been used to study a number of different biological outcomes, such as cellular differentiation, vascularization, or angiogenesis.<sup>3, 4</sup> These hydrogels can be formed by ultraviolet (UV) photocrosslinking of prepolymer solutions that contains the cells.

Photocrosslinking is a simple approach to induce the formation of 3D hydrogel networks. Photocrosslinkable hydrogels demonstrate a number of advantages compared to other stimuli. For instance, photocrosslinking is a cost-effective, rapid and simple way of fabricating 3D hydrogels with controlled shape, size, and spatial resolution.<sup>2</sup> Photocrosslinked cell-laden hydrogels have been successfully used for a number of applications, such as growth factor/drug delivery, regenerative medicine, and tissue engineering to study behavior of cells, for example proliferation, endothelialization, and stem cell differentiation.<sup>5-7</sup> A variety of cell-laden gels have been created by methacrylate functionalization of different polymers such as gelatin and HA and subsequent UV crosslinking of resultant polymer precursors.

HA is a non-adhesive<sup>8-11</sup>, non-thrombogenic<sup>12-14</sup> and non-immunogenic polymer. This anionic biopolymer consists of D-N-acetylglucosamine and D-glucuronic acid repeating units.<sup>15</sup> HA is a viscoelastic biomaterial and can be degraded by hyaluronidase enzyme.<sup>1, 2, 16-19</sup> HA is well-recognized as a major ECM component in a variety of tissues<sup>9</sup> such as central nervous system, connective, epithelial, cardiovascular tissues, cartilage as well as synovial and vitreous fluids. In addition, HA is an essential component in the formation of cardiac jelly while heart morphogenesis take place.<sup>20</sup> This polymer has been reported to play significant roles in wound healing, cellular proliferation, angiogenesis and cell-receptor interactions.<sup>1</sup> For instance, adhesion receptors, such as receptor for HA mediated motility (RHAMM), cluster of differentiation marker 44 (CD44) and intracellular adhesion molecule-1 (ICAM-1) possess binding affinities against HA.<sup>21, 22</sup> The carboxylate functional groups of HA can be chemically modified or methacrylated to facilitate crosslinking upon exposure to UV light.<sup>23</sup> Following this strategy, HA methacrylate (HAMA) can be synthesized at different methacrylation degrees to fabricate hydrogels with tunable physical properties including degradation, stiffness, and pore architecture.<sup>20</sup> Although HAMA is a promising hydrogel for biological applications, the nonadhesive nature prevents its use in applications where cell spreading is involved. The addition of gelatin with cell-interactive functional groups to the HA hydrogel matrix can improve cell adhesion properties of the resulting hybrid hydrogels.

Gelatin is traditionally obtained by partially hydrolyzing collagen and is composed of a heterogeneous mixture of proteins.<sup>23</sup> Collagen is the most substantial protein constituent of the tissues throughout the human body.<sup>24, 25</sup> For example, collagen is abundantly present in cartilage, bone, skin, ligament, tendon, heart, blood vessels, cornea, and epithelium.<sup>24</sup> Gelatin is a biocompatible material and has been used for coating of standard tissue culture dishes to promote cell adhesion for different cell types.<sup>26</sup> Furthermore, gelatin has been utilized for a number of small molecule delivery and tissue engineering applications.<sup>23, 27-35</sup> Gelatin degrades due to its matrix metalloproteinase (MMP) sensitive protein sequences, which is usually a desirable biomaterial property for *in vivo* implanted hydrogels. Degradation of tissue engineered constructs is essential for many applications in

regenerative medicine to allow for the deposition of newly formed ECM by the cells.<sup>36</sup> Cellular behavior (e.g. spreading, migration, differentiation) is strongly influenced by degradation properties of the scaffold, since scaffold degradation enables deposition and formation of new tissue. In some applications, scaffold degradation may also assist with controlled release of small molecules from the scaffold. The lysine functional groups on gelatin structure can be chemically modified or methacrylated to induce crosslinking upon exposure to UV light. Methacrylated gelatin (GelMA) is bioactive and it interacts with various cell lines.<sup>37</sup> Furthermore, GelMA allows the spreading of encapsulated cells due to its cell adhesive functional groups.<sup>37</sup> However, similar to collagen gels, UV-crosslinked gelatin hydrogels are mechanically weak.

Fabrication of hybrid hydrogels has been a popular approach to improve material and/or biological properties of biomaterials.<sup>1</sup> Although HA-gelatin hybrid hydrogels are promising biomimetic substrates<sup>38</sup>, their material properties have not been thoroughly characterized. In this study, we have used different compositions of HAMA and GelMA to generate tunable hybrid hydrogels and characterized their biological and mechanical properties. The physical properties of the resulting hydrogels, such as swelling, degradation and compressive moduli were controlled by varying prepolymer compositions prior to UV crosslinking. In addition, biological responses of human umbilical cord vein endothelial cells (HUVECs) to HAMA-GelMA hybrids were characterized by seeding cells on the hydrogel surfaces or encapsulating them within 3D structures of hybrids formed by using different compositions of HAMA and GelMA. Due to their abundance in the native ECM, HA and collagen/gelatin hybrids have great potential to be used for different tissue engineering applications (e.g. neural, bone, vascular, cardiac, skin) and regenerative medicine research.

## 2. MATERIAL AND METHODS

### 2.1. Materials

Methacrylic anhydride, Gelatin (type A, from porcine skin), and 3-(trimethoxysilyl) propyl methacrylate (TMSPMA) were obtained from Sigma-Aldrich (St Louis, MO). Pre-cleaned microscope slides were supplied by Fisher Scientific (Waltham, MA). Sodium hyaluronate was purchased from Lifecore Biomedical (Chaska, MN). The photoinitiator, 2-Hydroxy-1-[4-(hydroxyethoxy) phenyl]-2-methyl-1-propanone (Irgacure 2959), was purchased from Ciba Specialty Chemicals Corp. (Wilmington, MA, USA). A 16% (v/v) paraformaldehyde solution was obtained from Electron Microscopy Sciences (Hatfield, PA, USA). Dulbecco's phosphate buffered saline (DPBS), 4',6-diamidino-2-phenylindole (DAPI), alamarBlue, rhodamine phalloidin, trypsin-EDTA and penicillin-streptomycin were purchased from Invitrogen (Grand Island, NY, USA). Media for HUVECs and its components were obtained from Lonza Walkersville Inc. (Walkersville, MD, USA).

### 2.2. Synthesis of polymer precursors

GelMA was synthesized according to a procedure described previously.<sup>39</sup> Briefly, 10 grams of gelatin was combined with 100 mL DPBS at 50° C and stirred until fully dissolved. Eight mL of methacrylic anhydride was then added to dissolved gelatin solution and reacted for 3 h at 50°C. The resulting mixture was diluted with 300 mL DPBS to stop the methacrylation reaction. The solution was then dialyzed against distilled water for one week at 40 °C to remove unreacted reagents (12–14 kDa cut off dialysis membrane). The liquid mixture was lyophilized for seven days, frozen at –80 °C and freeze dried to obtain a solid product, which was maintained at –80 °C. The degree of methacrylation was determined as ~80% by <sup>1</sup>H NMR. HAMA was synthesized following a previously described procedure.<sup>40</sup> One gram of hyaluronic acid sodium salt was dissolved in 100 mL of distilled water until it fully dissolved. Methacrylic anhydride was then added to this solution at 1% (v/v) and the

reaction was performed for 24 h at 4 °C by maintaining the pH between 8–10 with the addition of 5 M sodium hydroxide. The resulting solution was dialyzed in 12–14 kDa dialysis membrane at 4 °C for 3 days, frozen at –80 °C and freeze dried to obtain a solid product, which was then kept at –80 °C until further use. The methacrylation degree was measured as ~20% by <sup>1</sup>H NMR.

### 2.3. Production of hybrid hydrogels

The prepolymer precursors (HAMA and GelMA) were mixed in DPBS at different compositions with 0.1% (w/v) photoinitiator (PI) and placed at 80 °C. GelMA prepolymers were prepared in the final concentrations of 0, 3, 5 and 10% (w/v), and HAMA solutions were prepared in the final concentrations of 0, 1 and 2% (w/v). The solutions were then briefly vortexed to obtain homogenous mixing. The solutions were kept in a 37 °C incubator until the UV crosslinking step.

### 2.4. Swelling analysis for hybrid hydrogels

To prepare the samples for swelling analysis, 100 uL prepolymer solution including 0.1% PI was placed between two untreated glass slides separated with a 1 mm spacer. The polymer mixture was then exposed to UV light (Omnire S2000, EXFO Photonic Solutions Inc., Ontario, Canada; wavelength 320–500 nm) for 90 sec at 2.5 mW/cm<sup>2</sup> power. Once the photopolymerization was complete, the unreacted polymer was rinsed by DPBS. The hydrogels discs were placed in eppendorf tubes which contained 1 mL DPBS for 24 h to reach equilibrium swelling. The wet weight of the swollen hydrogel disks was then determined after gently blotting the excess liquid by Kimwipes. This was followed by freezing and lyophilization steps to measure the dry weights of the hydrogels. The swelling ratio was determined by dividing wet weight with dry weight and the resulting number was converted into the corresponding percent (%) value. Four replicates were used for each hydrogel composition.

### 2.5. Degradation of hybrid hydrogels

The hybrid hydrogels for degradation study were produced as previously described for the swelling ratio analysis. Once removed from the glass slide, the hydrogels discs were rinsed with DPBS and placed in eppendorf tubes. The hydrogels were lyophilized and the initial weights were recorded. Dried hydrogels were then rehydrated in DPBS for 24 h. One mL of 2.5 U/mL of collagenase type II solution in DPBS was added on the hydrogels. They were then incubated at 37 °C on a shaker at 130 rpm and their degradation was analyzed at different points (4, 8, 12, 18, and 24 h). After removal of the enzyme solution, gels were rinsed with DPBS and lyophilized to determine the dry weight of remaining polymer. The percent mass remaining after degradation was calculated by dividing the dry weight after enzymatic degradation with the initial hydrogel weight and resulting numbers were converted into corresponding % values. Four replicates were used for each hydrogel composition.

### 2.6. Mechanical testing

The hybrid hydrogels for mechanical testing were produced as described in the swelling analysis section. After UV crosslinking, hydrogels were rinsed with DPBS and kept in DPBS for 24 h. The hydrogels were punched using an eight mm biopsy punch prior to mechanical testing. The excess liquid from the hydrogel disks was removed using Kimwipes. Compression testing was carried out by applying a strain rate of 0.2 mm/min using an Instron 5542 mechanical testing instrument. We determined the compressive modulus by taking the slope in the linear section of the stress-strain curve at 5%–10% strain area. Five replicates were used for each hydrogel composition.

## 2.7. Cell cultures

Green fluorescent protein (GFP) expressing human umbilical cord vein endothelial cells (HUVECs) were cultured in standard endothelial cell media supplemented by 1% (v/v) penicillin/streptomycin, 2% (v/v) fetal bovine serum (FBS), and the components of the Bullet kit. All HUVEC cultures were kept in a 37 °C incubator equipped to provide 5% CO<sub>2</sub>. The media was changed every two to three days.

## 2.8. Two dimensional (2D) cell adhesion on hybrid hydrogels

Hydrogel precursors containing different compositions of HAMA and GelMA (as given in Section 2.3) were prepared for 2D cell seeding experiments. To fabricate hybrid gels, 10 uL of prepolymer solution with desired composition was placed between a petri dish and a TMSPMA treated glass slide using 150 um spacers. This set up was exposed to ultraviolet (UV) light at 2.5 mW/cm<sup>2</sup> power for 30 or 120 sec. The crosslinked hydrogels were then kept in DPBS overnight after which, they were seeded with 0.6×10<sup>5</sup> HUVECs/cm<sup>2</sup> or 1.8×10<sup>5</sup> HUVECs/cm<sup>2</sup>. The non-adherent cells were rinsed by replacing media at day 1. The cell-seeded hydrogels were imaged at day 3 and then fixed by using 4% (v/v) paraformaldehyde for cytoskeleton/nuclei staining. Three replicates were used for each hydrogel composition.

## 2.9. Three dimensional (3D) cell encapsulation within hybrid hydrogels

Hydrogel precursor solutions with different compositions of HAMA and GelMA were prepared for 3D cell encapsulation as described in Section 2.3. Cells were trypsinized, centrifuged, counted and the desired number of HUVECs were placed in an eppendorf tube. The cell pellet was resuspended in the prepolymer solution to obtain a homogeneous cell suspension. To induce photocrosslinking, 10 uL of cell containing prepolymer solution was placed between a petri dish and a TMSPMA treated glass slide using 150 um spacers. Hydrogels were fabricated upon 30 sec exposure to (UV) light at 2.5 mW/cm<sup>2</sup> power. Subsequently, cell-laden hydrogels were rinsed with DPBS and cultured in endothelial media for a seven-day culture period. Samples were imaged at day 7 and then fixed with 4% (v/v) paraformaldehyde for cytoskeleton/nuclei staining. Three replicates were used for each hydrogel composition.

## 2.10. Alamar Blue assay

The Alamar Blue assay was performed by following manufacturer's protocols. The fluorescence values of resulting solutions were read at 544 nm/590 nm (Ex/Em) using a fluorescence plate reader (Fluostar GmbH, Offenburg, Germany). Three replicates were used for each hydrogel composition.

## 2.11. Statistical analysis

The statistical analyses were carried out by using GraphPad Prism (La Jolla, CA, USA). One-way and two-way ANOVA analyses were carried out in combination with Bonferroni tests. Data was represented as average ± standard deviation (\* $p < 0.05$ , \*\* $p < 0.01$ , and \*\*\* $p < 0.001$ ).

## 3. RESULTS AND DISCUSSION

We synthesized and characterized hybrid hydrogels composed of various ratios of HA and gelatin. These hybrid gels could potentially be used for a number of applications ranging from cardiovascular tissue engineering to stem cell differentiation. We characterized the physical properties of resulting hydrogels including swelling, degradation, compressive

moduli, as well as biological properties such as cell adhesion affinity in 2D culture and cell spreading behavior within the 3D gels.

HA and collagen are major native ECM components in various tissues. However, when used as single component biomaterials they demonstrate several drawbacks. For example, although HA is a major ECM component, its non-adhesive nature limits its use in the applications where cell spreading is required. The limitation of gelatin hydrogels is mainly due to their mechanical weakness and quick degradation behavior. To improve the physical and biological properties of HAMA and GelMA, we fabricated HAMA-GelMA hybrid hydrogels using different ratios of these two components.

### 3.1. Swelling of hybrid hydrogels

Hydrogels contain more than 90% water and have the ability to maintain it in their 3D crosslinked structures.<sup>2, 41</sup> Swelling ability of hydrogels is an indication of the degree of hydrophilicity and is influenced by hydrogel pore size.<sup>37</sup> This unique feature has been shown to influence cellular behavior.<sup>41</sup>

In this study, the swelling behavior of HAMA-GelMA hybrid hydrogels was found to be tunable by varying the composition of the gel components (Figure 1). For example, the addition of 1% (w/v) HAMA into all concentrations of GelMA hydrogels significantly decreased the mass swelling ratio ( $p < 0.001$ ). The swelling ratio decreased from  $28.6 \pm 1.7$  in a 3% GelMA to  $20.5 \pm 0.9$  in a hybrid gel containing 1% HAMA and 3% GelMA. Similarly, a significant decrease was observed upon comparison of 1% HAMA and 1% HAMA-10% GelMA conditions ( $p < 0.001$ ). These results were expected, because increasing polymer concentration allows for higher crosslinking density as previously reported.<sup>42, 43</sup> Therefore, the resulting hydrogels possess smaller pore size and induce less swelling compared to that of lower polymer concentrations. When we further increase the concentration of HAMA to 2% (w/v), it did not significantly change the mass swelling ratio of the hybrid hydrogels when compared to the conditions with 1% HAMA. Additionally, we determined the influence of polymer concentration on the swelling ratio of hydrogels with single components. To demonstrate this, we excluded HAMA from GelMA hydrogels and found out that water swelling ratio decreased from  $28.6 \pm 1.7$  to  $8.0 \pm 0.3$  by increasing the GelMA concentration from 3% to 10% (w/v). Similarly, when GelMA was not included in HAMA hydrogels, increasing concentration of HAMA caused a significant decrease in mass swelling ratio ranging from  $52.2 \pm 5.1$  to  $39.0 \pm 1.2$  for 1% and 2% HAMA conditions respectively. These results point out that HAMA-GelMA hybrid hydrogels exhibit tunable swelling behavior.

### 3.2. Degradation of hybrid hydrogels

Engineered hydrogel-based scaffolds are often designed to degrade within the body following implantation at a rate similar to the rate of tissue formation. Hydrogel degradation at physiological conditions is advantageous because this allows for the scaffold to disappear, thus the new ECM slowly can fill out the degraded portions of the hydrogel. Degradation of hydrogels can be induced by the use of enzymes, chemicals, or water-sensitive functional groups.<sup>41</sup> For example, collagenase is a natural enzyme that degrades collagen.<sup>44</sup>

To assess how polymer composition alters degradation behavior, we studied enzymatic degradation of HAMA-GelMA hydrogel mixtures by collagenase, which degrades the GelMA component (Figure 2). We used 2.5 U/mL collagenase to study degradation trend of HAMA-GelMA hydrogels at 37 °C under shaking conditions at 130 rpm. The increase in the concentration of GelMA resulted in slower gel degradation as expected. The 3% GelMA hydrogels were completely degraded after 12 h exposure to 2.5 U/ml collagenase at 37 °C,

whereas it took 24 h for 5% GelMA to achieve complete degradation. On the other hand, more than half of the mass was remained for 10% GelMA was after 24 h enzymatic degradation ( $55.7 \pm 3.1\%$ ). It has been shown that the enzymatic degradation of hydrogels and their stiffnesses are correlated.<sup>45</sup> Our results were in agreement with this observation, degradation rate increased as the stiffness of the hydrogel decreased.

To study the effect of gel composition on degradation of hybrid hydrogels, we followed the same experimental procedure as explained above for single component gels. The addition of 1% HAMA into 3, 5 or 10% GelMA resulted in a significant decrease in degradation rate ( $p < 0.001$ ). This may be due to the addition of a second polymer (HAMA), which is not degraded by collagenase type II, significantly slowing down the degradation compared to single network GelMA hydrogels ( $p < 0.001$ ). When the amount of HAMA was increased to 2% (w/v), degradation of HAMA-GelMA hydrogels further decreased for 3 and 5% GelMA conditions in the hybrid gel network. There was no significant difference between the gel degradation of 1% HAMA-10% GelMA and 2% HAMA-10% GelMA, potentially because of the higher concentration of GelMA compared to the rest of the conditions. The enzymatic degradation of 10% GelMA is slower compared to 3% and 5% making it even harder to degrade the hydrogel mixture with increasing HAMA concentrations. Collectively, these experiments demonstrated the tunable degradation behavior of HAMA-GelMA hydrogels by collagenase.

### 3.3. Mechanical properties of hybrid hydrogels

Mechanical properties of hydrogels are influenced by the crosslinking density of the polymer networks.<sup>41</sup> Mechanical properties significantly affect the spreading behavior of cells in both 2D and 3D. For example, substrate stiffness has been shown to be important for modulation of cellular behavior, such as regulation of phenotypes.<sup>46–48</sup> As reported earlier, the stiffness of hydrogels is inversely proportional to their pore sizes.<sup>49</sup> Therefore, cells do not spread within 3D if the pore size of the biomaterial is too small.<sup>50</sup>

The material stiffness enhances as the polymer concentration increase, which results in an increase in the mechanical properties.<sup>51</sup> We observed the same trend in our experiments as supported by other studies.<sup>37, 49</sup> The compressive moduli were determined to be  $0.9 \pm 0.2$  kPa,  $3.4 \pm 2.1$  kPa, and  $33.6 \pm 23.2$  kPa for 3, 5 and 10% GelMA, respectively (Figure 3). Similarly, increasing HAMA concentration from 1% to 2% caused an increase in the compressive moduli from  $1.5 \pm 0.4$  to  $3.8 \pm 1.0$  kPa ( $p < 0.001$ ). Based on these results, there is a significant effect of polymer concentration on compressive moduli as expected. The addition of a second polymer (1% or 2% HAMA) to 3% GelMA hydrogels significantly enhanced the compressive moduli ( $p < 0.001$ ). Similarly, when the GelMA concentration was further increased to 10%, the addition of 2% HAMA resulted in a significant increase in the compressive moduli from  $33.6 \pm 23.2$  kPa to  $73.0 \pm 11.1$  kPa.

Overall, HAMA-GelMA hybrid hydrogels were determined to be mechanically tunable compressive moduli ranging from  $1.5 \pm 0.4$  to  $73.0 \pm 11.1$  kPa, which could be useful for a number of different tissue engineering applications such as, neural, cardiac, cardiovascular, cartilage or skeletal muscle due to having similar mechanical values to native tissues.<sup>52–54</sup>

### 3.4. 2D cell adhesion on hybrid hydrogels

Chemical nature of the hydrogel constituents affects the cytotoxicity behavior in 2D cell seeding studies.<sup>41</sup> Cell adhesion on 2D surfaces changes with respect to material stiffness and biological functional groups on the substrate.<sup>55</sup> Substrate stiffness can also alter other cellular behavior, for example it may induce changes in cellular phenotype.<sup>43</sup> Stiffness can be tuned by changing the crosslinking density of the polymeric material.<sup>55</sup>

In this study, we quantified spreading of HUVECs on HAMA-GelMA hybrid hydrogels by calculating % area occupied by the cells at day 3 of culture. To demonstrate biological tunability of these hydrogels, we used different UV exposure times and cell seeding densities (Figure 4). First, we generated hybrid hydrogels by exposing them for 30 sec to UV to induce crosslinking. These gels were then seeded with  $0.6 \times 10^5$  HUVECs per  $\text{cm}^2$ . Cell adhesion to these hydrogels was low enabling a maximum  $3.0 \pm 0.4\%$  confluency upon 3 days in culture. The hydrogels that are composed of only HAMA, neither 1% nor 2% (w/v), did not induce cell adhesion and therefore no HUVEC spreading was observed on them. On the other hand, the addition of GelMA improved cell spreading affinity due to its cell adhesive functional groups. The increase in GelMA concentration also enhanced the hybrid hydrogel stiffness and improved cell spreading behavior as expected.<sup>45, 56, 57</sup> Second, we increased the crosslinking time to 120 sec and kept the cell seeding density constant. The increase in the UV crosslinking time resulted in formation of significantly stiffer hydrogels, which greatly enhanced the cell spreading ( $p < 0.001$ ). As a result, maximum level of % confluency was increased to  $10.1 \pm 2.0$  with a similar trend consistent with the previous observation. Finally, we increased the cell seeding density to  $1.8 \times 10^5$  HUVECs per  $\text{cm}^2$  by maintaining the UV exposure time at 120 sec. As expected, HUVEC spreading was significantly increased for all concentrations of the hybrid hydrogels with a maximum level of confluency at  $58.8 \pm 6.7\%$ . However, for 1% and 2% HAMA hydrogels neither the increase in cell seeding density nor UV exposure time affected the confluency at day 3 because of the non-adhesive properties of HAMA. In summary, HAMA-GelMA hydrogels demonstrated tunable cell adhesion behavior when HUVECs were seeded on them in 2D.

### 3.5. 3D cell encapsulation within hybrid hydrogels

Biomaterial properties significantly influence cellular behavior when encapsulated within 3D networks. For example, crosslinking density within a cell-laden hydrogel matrix may influence the cytotoxicity behavior.<sup>40, 41</sup> Similarly, cellular spreading depends on the biofunctional groups on the material and the stiffness of the substrate.<sup>41</sup>

We observed that HUVECs encapsulated in nonadhesive HAMA hydrogels had no spreading within 3D structure of the gel. The addition of GelMA into 1% and 2% HAMA hydrogels resulted in a significant increase in cell spreading in 3D constructs. Unlike the 2D results, increasing hydrogel stiffness decreased the spreading ability of the cells in 3D environments (Figure 5). This could be due to the fact that increasing hydrogel stiffness decreases the pore size, which limits the space for cellular elongation, spreading and migration.<sup>49, 50</sup> The highest degree of spreading was observed for HUVECs encapsulated within 3% (w/v) GelMA hydrogels. This is potentially due to the cell adhesive functional groups on GelMA and larger pore size of the hydrogel construct compared to the rest of the conditions. The addition of 1% non-adhesive HAMA allowed for cell spreading to an extent suggesting potential applications in different tissue engineering areas (Figure 6). A further increase in HAMA concentration to 2%, reduced the 3D cell spreading to a greater extent. Similarly, as the GelMA concentration was increased cell spreading significantly decreased. Overall, HAMA-GelMA hydrogels demonstrated tunable 3D cell spreading within the hybrid hydrogels. The results pointed out that by changing the concentration of HA or gelatin component, it is possible to fabricate hybrid hydrogels with different stiffnesses that allows for tunable cellular response.

In addition to spreading affinity of HUVECs, we also tested proliferation of these cells within HAMA-GelMA hybrids (Figure 7). Proliferation of cells depends on the cell spreading and stiffness of the substrate in both 2D and 3D.<sup>58, 59</sup> In 2D, increasing cell spreading enhances proliferation.<sup>45</sup> However, it has been shown that 3D proliferation reduced with increasing hydrogel stiffness.<sup>44</sup> Our observation is in agreement with this



finding, as we found that proliferation has significantly decreased when substrates stiffness increased ( $p < 0.001$ ).

#### 4. CONCLUSIONS

Methacrylated HA and gelatin were successfully used to generate hybrid hydrogels using different concentrations of HA and gelatin. We have determined the material properties of the resulting hybrid hydrogels and assessed the cellular response in both 2D and 3D. The physical and biological properties of these hydrogels were characterized and found that they can be biologically and mechanically tuned to yield in a range of different cellular response for HUVECs. The addition of GelMA with cell-interactive functional groups into HAMA induced cellular spreading in the HAMA-containing hybrid hydrogels offering new opportunities to develop novel biomaterials. Similarly, hydrogels that were generated by the addition of HAMA into GelMA, demonstrated significantly higher mechanical properties compared to their single component analogs. The ability to precisely control physical and biological properties of engineered constructs may enable generation of reliable off-the-shelf tissue products in the future. Due to their abundance in the native ECM, HA and collagen/gelatin hybrids have great potential to be used for various biomedical applications, ranging from drug delivery and cell transplantation to tissue engineering.

#### Acknowledgments

This paper was supported by the Office of Naval Research Young National Investigator Award, the Presidential Early Career Award for Scientists and Engineers (PECASE), the National Institutes of Health (HL092836, AR057837, DE021468, HL099073, DE019024, EB012597, EB008392), and the National Science Foundation CAREER Award (DMR 0847287).

#### References

1. Peppas NA, Hilt JZ, Khademhosseini A, Langer R. Hydrogels in biology and medicine: From molecular principles to bionanotechnology. *Adv Mater.* 2006; 18:1345–1360.
2. Slaughter BV, Khurshid SS, Fisher OZ, Khademhosseini A, Peppas NA. *Adv Mater.* 2009; 21:3307–3329. [PubMed: 20882499]
3. Mann B, Gobin A, Tsai A, Schmedlen R, West J. *Biomaterials.* 2001; 22:3045–3051. [PubMed: 11575479]
4. Kaji H, Camci-Unal G, Langer R, Khademhosseini A. *Biochim Biophys Acta, Gen Subj.* 2011; 1810:239–250.
5. Zhong C, Wu J, Reinhart-King CA, Chu CC. *Acta Biomater.* 2010; 6:3908–3918. [PubMed: 20416406]
6. Gerecht S, Burdick JA, Ferreira LS, Townsend SA, Langer R, Vunjak-Novakovic G. *Proc Natl Acad Sci USA.* 2007; 104:11298–11303. [PubMed: 17581871]
7. Lozoya OA, Wauthier E, Turner RA, Barbier C, Prestwich GD, Guilak F, Superfine R, Lubkin SR, Reid LM. *Biomaterials.* 2011; 32:7389–7402. [PubMed: 21788068]
8. Manasek FJ. *Circ Res.* 1976; 38:331–337. [PubMed: 131651]
9. Tian WM, Zhang CL, Hou SP, Yu X, Cui FZ, Xu QY, Sheng SL, Cui H, Li HD. *J Controlled Release.* 2005; 102:13–22.
10. Markwald RR, Fitzharris TP, Bernanke DH. *J Histochem Cytochem.* 1979; 27:1171–1173. [PubMed: 479561]
11. Camci-Unal G, Nichol JW, Bae H, Tekin H, Bischoff J, Khademhosseini A. *J Tissue Eng Regen Med.* 2012;10.1002/term.517
12. Mason M, Vercruyse KP, Kirker KR, Frisch R, Marecak DM, Prestwich CD, Pitt WG. *Biomaterials.* 2000; 21:31–36. [PubMed: 10619676]
13. Verheye S, Markou CP, Salame MY, Wan B, King SB, Robinson KA, Chronos NAF, Hanson SR. *Arterioscler, Thromb, Vasc Biol.* 2000; 20:1168–1172. [PubMed: 10764689]

14. Masters KS, Shah DN, Walker G, Leinwand LA, Anseth KS. *J Biomed Mater Res, Part A*. 2004; 71A:172–180.
15. Coradini D, Pellizzaro C, Miglierini G, Daidone MG, Perbellini A. *Int J Cancer*. 1999; 81:411–416. [PubMed: 10209956]
16. Suri S, Schmidt CE. *Acta Biomater*. 2009; 5:2385–2397. [PubMed: 19446050]
17. Lei YG, Gojgini S, Lam J, Segura T. *Biomaterials*. 2011; 32:39–47. [PubMed: 20933268]
18. Ji Y, Ghosh K, Shu XZ, Li BQ, Sokolov JC, Prestwich GD, Clark RAF, Rafailovich MH. *Biomaterials*. 2006; 27:3782–3792. [PubMed: 16556462]
19. Fujie T, Furutate S, Niwa D, Takeoka S. *Soft Matter*. 2010; 6:4672–4676.
20. Masters KS, Shah DN, Leinwand LA, Anseth KS. *Biomaterials*. 2005; 26:2517–25. [PubMed: 15585254]
21. Matou-Nasri S, Gaffney J, Kumar S, Slevin M. *Int J Oncol*. 2009; 35:761–773. [PubMed: 19724912]
22. Braun M, Pietsch P, Schror K, Baumann G, Felix SB. *Cardiovasc Res*. 1999; 41:395–401. [PubMed: 10341839]
23. Benton JA, DeForest CA, Vivekanandan V, Anseth KS. *Tissue Eng, Part A*. 2009; 15:3221–30. [PubMed: 19374488]
24. Parenteau-Bareil R, Gauvin R, Berthod F. *Materials*. 2010; 3:1863–1887.
25. Pataridis S, Eckhardt A, Mikulikova K, Sedlakova P, Miksik I. *Curr Anal Chem*. 2009; 5:316–323.
26. Sreejit P, Kumar S, Verma RS. *In Vitro Cell Dev Biol: Anim*. 2008; 44:45–50. [PubMed: 18297366]
27. Adhirajan N, Shanmugasundaram N, Shanmuganathan S, Babu M. *Eur J Pharm Sci*. 2009; 36:235–245. [PubMed: 18952165]
28. Chen TH, Embree HD, Brown EM, Taylor MM, Payne GF. *Biomaterials*. 2003; 24:2831–2841. [PubMed: 12742721]
29. Kimura Y, Ozeki M, Inamoto T, Tabata Y. *Biomaterials*. 2003; 24:2513–2521. [PubMed: 12695078]
30. Kommareddy S, Amiji M. *Bioconjugate Chem*. 2005; 16:1423–32.
31. Kosmala JD, Henthorn DB, Brannon-Peppas L. *Biomaterials*. 2000; 21:2019–2023. [PubMed: 10966010]
32. Kuijpers AJ, Engbers GHM, Feijen J, De Smedt SC, Meyvis TKL, Demeester J, Krijgsveld J, Zaat SAJ, Dankert J. *Macromolecules*. 1999; 32:3325–3333.
33. Liu Y, Chan-Park MB. *Biomaterials*. 2010; 31:1158–1170. [PubMed: 19897239]
34. Huang Y, Onyeri S, Siewe M, Moshfeghian A, Madihally SV. *Biomaterials*. 2005; 26:7616–7627. [PubMed: 16005510]
35. Young S, Wong M, Tabata Y, Mikos AGJ. *Controlled Release*. 2005; 109:256–274.
36. Drury JL, Mooney DJ. *Biomaterials*. 2003; 24:4337–4351. [PubMed: 12922147]
37. Nichol JW, Koshy ST, Bae H, Hwang CM, Yamanlar S, Khademhosseini A. *Biomaterials*. 2010; 31:5536–5544. [PubMed: 20417964]
38. Camci-Unal G, Aubin H, Ahari AF, Bae H, Nichol JW, Khademhosseini A. *Soft Matter*. 2010; 6:5120–5126. [PubMed: 22368689]
39. Ahadian S, Ramon-Azcon J, Ostrovidov S, Camci-Unal G, Hosseini V, Kaji H, Ino K, Shiku H, Khademhosseini A, Matsue T. *Lab Chip*. 2012; 12:3491–3503. [PubMed: 22847280]
40. Burdick JA, Chung C, Jia XQ, Randolph MA, Langer R. *Biomacromolecules*. 2005; 6:386–391. [PubMed: 15638543]
41. Shi J, Xing MMQ, Zhong W. *Membranes*. 2012; 2:70–90.
42. Tong X. *Mater Lett*. 2007; 61:1704–1706.
43. Cha C, Kim SY, Cao L, Kong H. *Biomaterials*. 2010; 31:4864–4871. [PubMed: 20347136]
44. Wang L-S, Chung JE, Pui-Yik Chan P, Kurisawa M. *Biomaterials*. 2010; 31:1148–1157. [PubMed: 19892395]
45. Wang LS, Boulaire J, Chan PPY, Chung JE, Kurisawa M. *Biomaterials*. 2010; 31:8608–8616. [PubMed: 20709390]

46. Anseth KS, Bowman CN, Brannon-Peppas L. *Biomaterials*. 1996; 17:1647–1657. [PubMed: 8866026]
47. Geiger B, Spatz JP, Bershadsky AD. *Nat Rev Mol Cell Biol*. 2009; 10:21–33. [PubMed: 19197329]
48. Brandl F, Sommer F, Goepferich A. *Biomaterials*. 2007; 28:134–146. [PubMed: 17011028]
49. Chen YC, Lin RZ, Qi H, Yang Y, Bae H, Melero-Martin JM, Khademhosseini A. *Adv Funct Mater*. 2012; 22:2027–2039. [PubMed: 22907987]
50. Sant S, Hancock MJ, Donnelly JP, Iyer D, Khademhosseini A. *Can J Chem Eng*. 2010; 88:899–911. [PubMed: 21874065]
51. Nam K, Watanabe J, Ishihara K. *Eur J Pharm Sci*. 2004; 23:261–270. [PubMed: 15489127]
52. Seidlits SK, Khaing ZZ, Petersen RR, Nickels JD, Vanscoy JE, Shear JB, Schmidt CE. *Biomaterials*. 2010; 31:3930–3940. [PubMed: 20171731]
53. Cimetta E, Pizzato S, Bollini S, Serena E, De Coppi P, Elvassore N. *Biomed Microdevices*. 2009; 11:389–400. [PubMed: 18987976]
54. Park Y, Lutolf MP, Hubbell JA, Hunziker EB, Wong M. *Tiss Eng*. 2004; 10:515–522.
55. Hule RA, Nagarkar RP, Altunbas A, Ramay HR, Branco MC, Schneider JP, Pochan DJ. *Faraday Discuss*. 2008; 139:251–264. [PubMed: 19048999]
56. Ghosh K, Pan Z, Guan E, Ge SR, Liu YJ, Nakamura T, Ren XD, Rafailovich M, Clark RAF. *Biomaterials*. 2007; 28:671–679. [PubMed: 17049594]
57. Engler AJ, Sen S, Sweeney HL, Discher DE. *Cell*. 2006; 126:677–689. [PubMed: 16923388]
58. Folkman J, Moscona A. *Nature*. 1978; 273:345–349. [PubMed: 661946]
59. Chen CS, Mrksich M, Huang S, Whitesides GM, Ingber DE. *Science*. 1997; 276:1425–1428. [PubMed: 9162012]

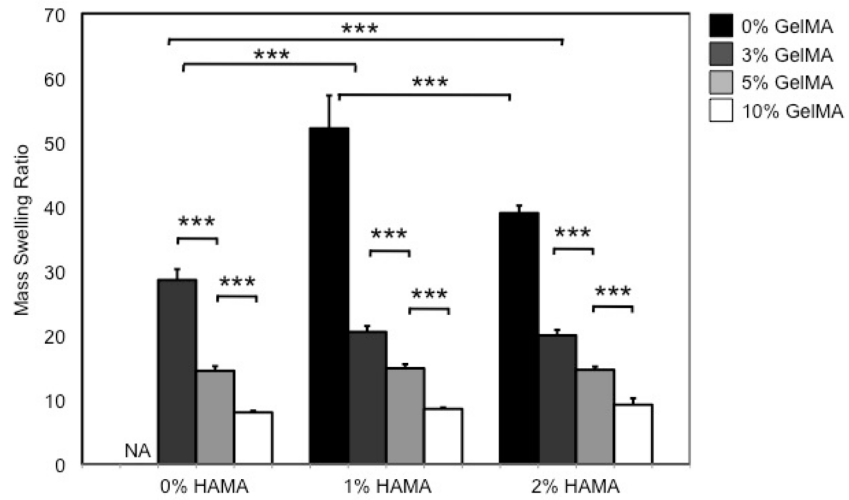


**Figure 1.** Mass swelling ratio of HAMA-GelMA hybrid hydrogels at different concentrations. The swelling behavior of HAMA-GelMA hybrid hydrogels was tunable (NA: Not applicable, error bars:  $\pm$ SD, \*\*\* $p$ <0.001).

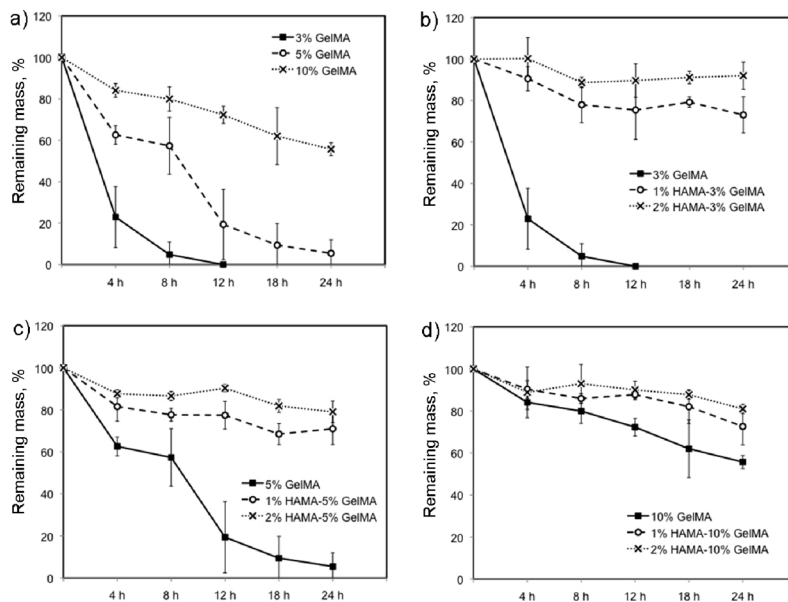


**Figure 2.** Degradation of HAMA-GelMA hybrid hydrogels at different concentrations by 2.5 U/mL collagenase. The increase in the concentration of GelMA degrades the gels slower demonstrating the tunable degradation behavior of HAMA-GelMA hybrid hydrogels.

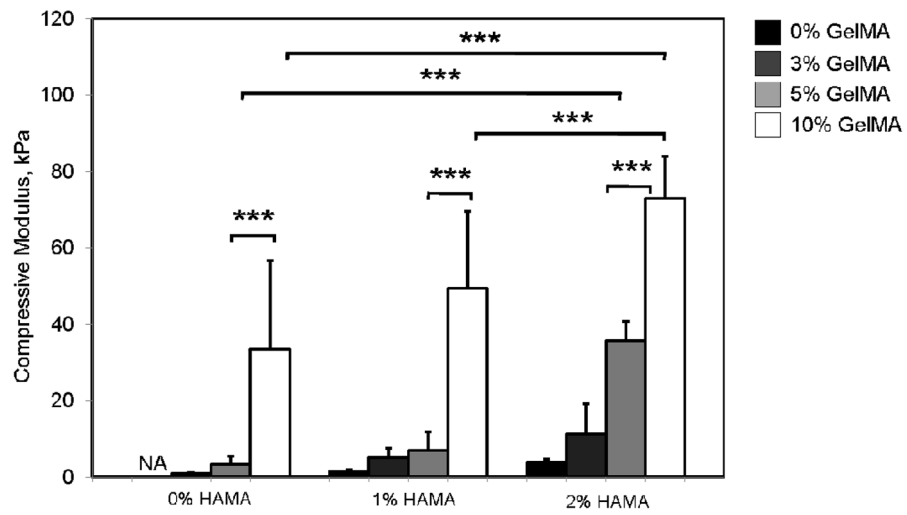


**Figure 3.** Mechanical characterization of HAMA-GelMA hybrid hydrogels at different concentrations. The compressive moduli for HAMA-GelMA hybrid hydrogels are found to be mechanically tunable (NA: Not applicable, error bars:  $\pm$ SD, \*\*\* $p$ <0.001).

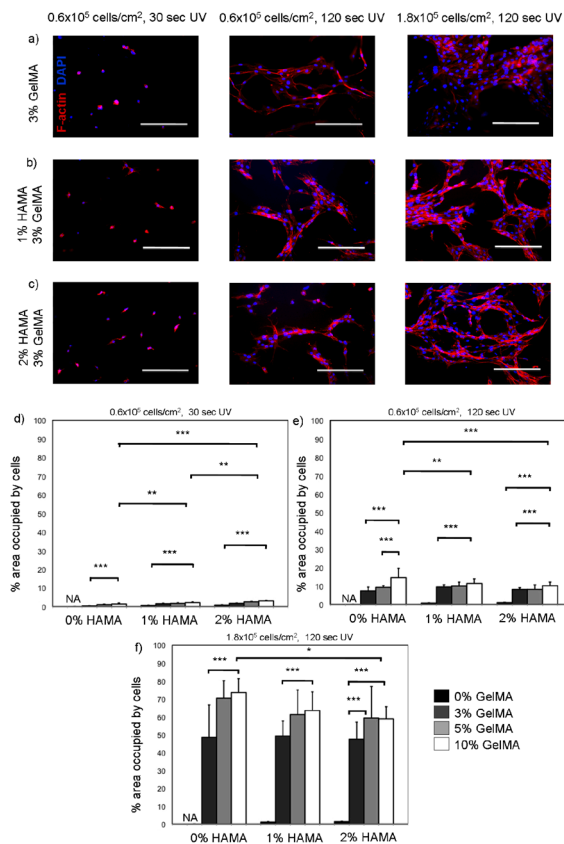


**Figure 4.** Cytoskeleton and nuclei staining (F-actin/DAPI) for HUVEC-seeded HAMA-GelMA hybrid hydrogels in 2D and quantification of cell spreading on the hybrid hydrogels. Percent (%) area occupied by the cells on day 3 was calculated at different conditions. a-c) The hydrogels were crosslinked at different UV exposure times and seeded with different cell densities to study tunability of cell spreading (data is taken at day 3). Scale bars represent 100  $\mu$ m; d) UV time: 30 sec, cell density:  $0.6 \times 10^5$  cells/cm<sup>2</sup>; e) UV time: 120 sec, cell density:  $0.6 \times 10^5$  cells/cm<sup>2</sup>; f) UV time: 120 sec, cell density:  $1.8 \times 10^5$  cells/cm<sup>2</sup> (NA: Not applicable, error bars:  $\pm$ SD, \*  $p < 0.05$ , \*\*  $p < 0.01$ , and \*\*\*  $p < 0.001$ ).

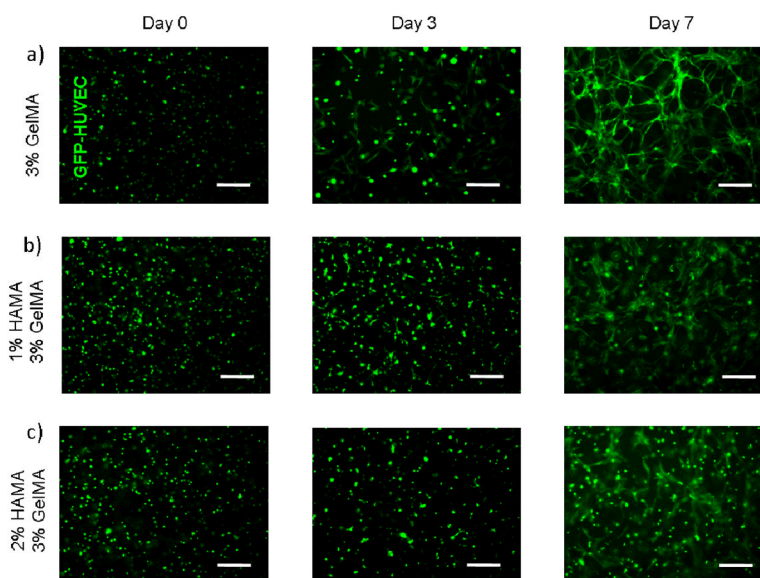


**Figure 5.** Fluorescent imaging for HUVEC-laden HAMA-GelMA hybrid hydrogels in 3D. Cell spreading data is given for days 0, 3, and 7. Scale bars represent 100  $\mu$ m.



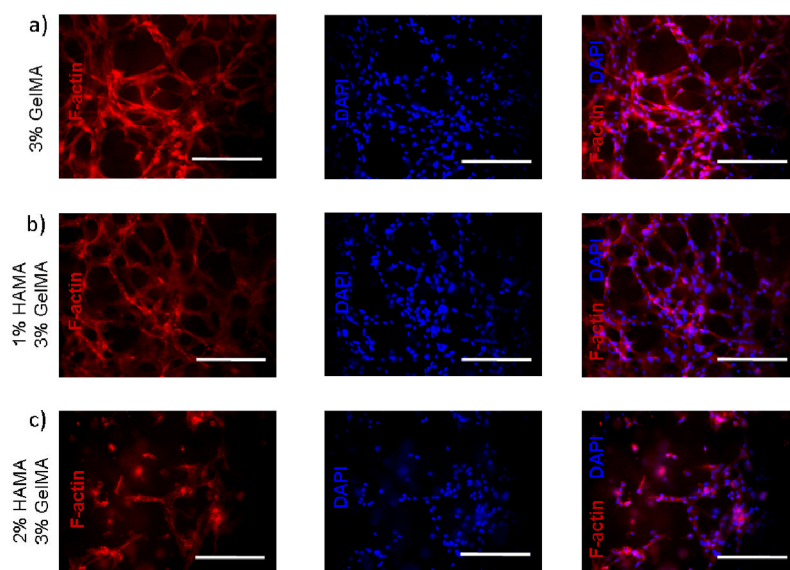


**Figure 6.** Cytoskeleton and nuclei staining (F-actin/DAPI) for HUVEC-laden HAMA-GelMA hybrid hydrogels in 3D. Cell spreading images are taken at day 7. Scale bars represent 100  $\mu$ m.

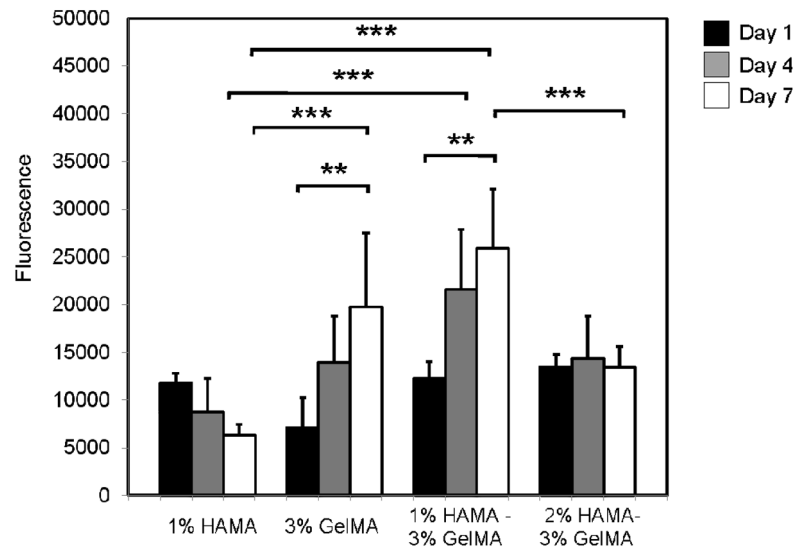


**Figure 7.** Proliferation of HUVECs within HAMA-GelMA hybrid hydrogels at different hydrogel conditions. Alamar Blue values are provided as the fluorescence reading at 544/590 nm (Ex/Em) (error bars:  $\pm$ SD, \*\* $p$ <0.01, and \*\*\* $p$ <0.001).